ORIGINAL ARTICLE

CrossMark

The surface chemical constituent analysis of poplar fibrosis veneers during heat treatment

Yanan Wei[1] · Yuxiang Huang[1] · Yanglun Yu[1] · Ruiqing Gao[1] · Wenji Yu[1]

Abstract

The scrimber is composed of the special elementary unit called fibrosis veneers. Study on chemical constituent changes of fibrosis veneers during heat treatment is helpful to expand the application areas of scrimbers. The objectives of this study were to investigate the effect of heat treatment on the chemical composition of poplar fibrosis veneers. The content changes of chemical composition and extractives after heat treatment were evaluated by chemical analysis. X-ray photoelectron spectroscopy (XPS) and solid-state nuclear magnetic resonance (NMR) were used to characterize the changes in the chemical structure of components. Untreated samples were also set for comparison. The results indicated that transformation of the material induced by this treatment led to an increase in the contents of lignin and extractives, while a decrease in those of holocellulose and α-cellulose. XPS spectroscopy results showed that the hemicelluloses and celluloses could be strongly affected by the atmosphere in the oven during the treatment. Relatively, the lignin was not very sensitive to the heating process to some extent. Solid-state NMR results showed that different degrees of transformations of the polymers took place during the heat treatment, resulting from the deacetylation of hemicelluloses, demethoxylation of lignin and changes in the cellulose structure.

Keywords Fibrosis veneers · Thermal treatment · Chemical constituents · Nuclear magnetic resonance (NMR) · XPS spectroscopy

Introduction

The scrimber is generally composed of fiber bundle of inferior quality material such as poplar, eucalyptus etc., [1–5]. The fibrosis treatment in the manufacturing process of the scrimber is carried on the thick veneer using fluffing and separation technique, which is essentially different from the traditional manufacture technology of wood products. The fiber bundles which were mutually connected together and kept the initial arranged orientation were impregnated with low-molecular polymer as adhesive to manufacture the scrimber. Compared with other poplar wood products [6–9], the scrimber has higher mechanical properties and raw material utilization rate. Hence, it is an effective way to develop value added utilizations of fast-growing materials such as poplar.

Heat treatment, known as a conventional method of physical treatment to wood, has been widely studied and used. Treating wood at temperatures above 150 °C leads to more or less intense chemical transformations of the polymers of the cell wall [10], such as hemicelluloses decomposition [11], lignin ramification [12] and cellulose crystallization [13] as well as volatilization of water and organic volatile components with low-molecular weight [14]. As a result, the water resistance and dimensional stability of wood are improved, and the surface color of wood deepens. Attentions have been focused on heat-treated elementary unit of wood products to improve product properties. A previous research

✉ Wenji Yu
   chinayuwj@126.com

   Yanan Wei
   490424060@qq.com

   Yuxiang Huang
   yxhuang@caf.ac.cn

   Yanglun Yu
   yuyanglun@caf.ac.cn

   Ruiqing Gao
   ray@caf.ac.cn

1 Research Institute of Wood Industry, Chinese Academy of Forestry, Xiang Shan Road, Hai Dian District, Beijing 100091, People's Republic of China

demonstrated that particleboards prepared from heat-treated chips have reduced hydrophilic properties [15]. Similar results have been discovered for medium density fibreboard (MDF) produced from heat-treated fibres [16]. However, whether the various properties of scrimbers produced from thermally treated fibrosis veneers are changed has not been explored. Therefore, it is necessary to study the effect of heat treatment on the performance of fibrosis veneers, which is of considerable importance in considering the properties of the final products. On the other hand, although a lot of data are available about the heat treatment process, color change, dimensional stability, mechanical property and durability of heat-treated wood [17–19], relatively little research has addressed alteration mechanism of the chemical composition of heat-treated wood surface [20]. That is the crucial factor in determining the operating conditions of the treatment and provides a better understanding of the chemical and physical transformations occurring in the material. Therefore, it is quite necessary to study the transformation process of the chemical composition of fibrosis veneers.

The objective of this work was to investigate the surface chemical structure of fibrosis veneers (poplar) during the heat treatment under the specified condition using X-ray photoelectron spectroscopy (XPS) and solid-state nuclear magnetic resonance (NMR) analytical technique.

Experimental

Fibrosis veneers production

Hybrid poplar logs with a diameter of approximately 20 cm were obtained from the Shandong province of China, aged for 10 years. The poplar log was sawn into 1200 mm long and then ratably cut into veneers with a thickness of 8 mm. The veneers with the moisture of 35–40% were fibered by the special machinery to obtain fibrosis veneers. Fibrosis degree of poplar veneers was evaluated by the diameter range of poplar fiber bundles, the range of which was 1.5–2.5 mm (seen Fig. 1). In addition, the microstructure morphological features
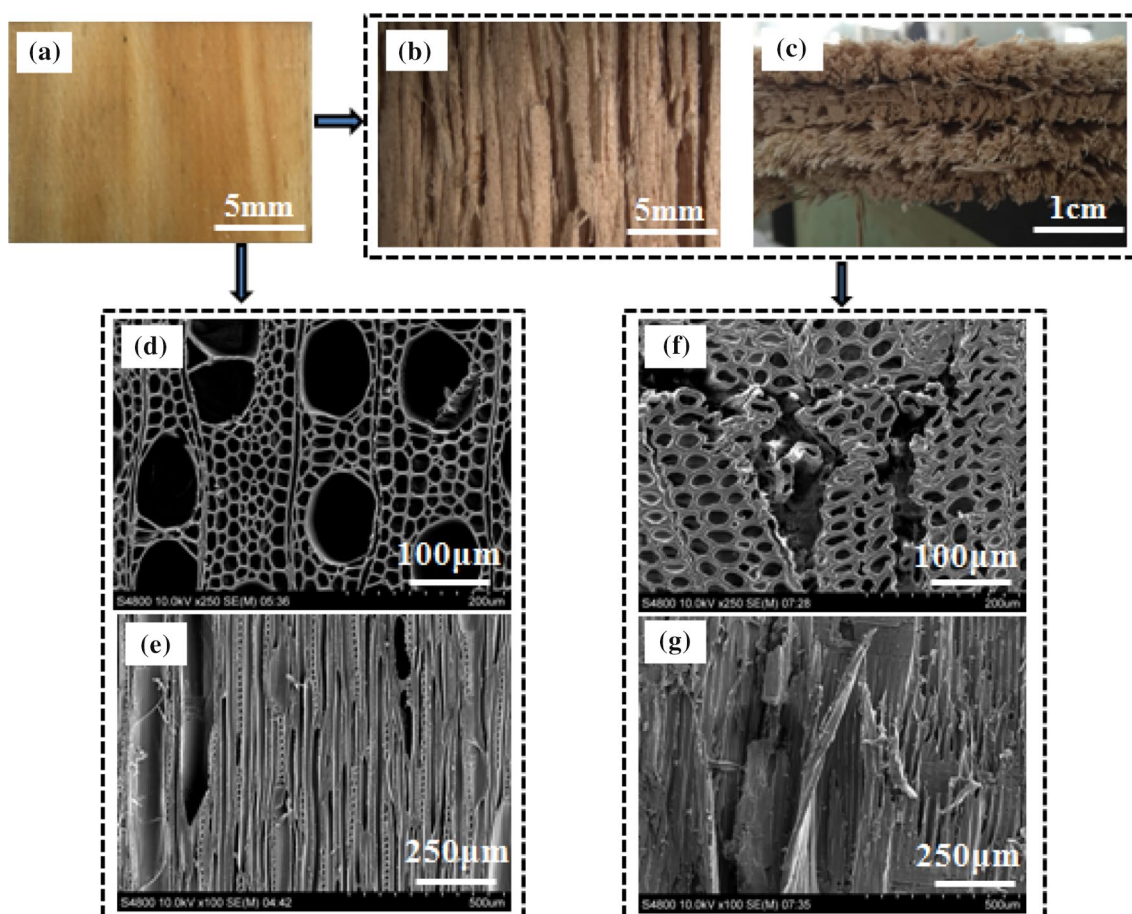
Fig. 1 The pictures of untreated poplar veneers and fibrosis veneers. a Thick poplar veneers. b Fibrosis veneers. c The transverse section of fibrosis veneers. d, e SEM micrographs on transverse/tangential section of untreated hybrid poplar. f, g SEM micrographs on transverse/tangential section of fibrosis veneers

of veneers and fibrosis veneers were observed with scanning electron microscope (SEM) producing micrographs. The samples were cut randomly from veneers and fibrosis veneers using microtome, and then baked in a hot oven for 4 h to oven dry. The dry samples were mounted on conductive adhesive tapes. Then, the cutting surfaces were sputter-coated gold and scanned in SEM with the magnification of up to 100×.

Heat treatment

The above fibrosis veneers were dried at the temperature 35–40 °C to achieve a moisture content of 6–7% for further treatment. According to preliminary experiments and previous researches, heat treatment was carried out at 160 °C/0.3 MPa and 180 °C/0.3 MPa for 2 h under steam pressure in a heat treatment oven, during which the oxygen content was controlled at 2.5% (Jiangyin xingnan Pressure Vessel Co., Ltd., Jiangsu, China). As was mentioned above, the initial moisture content of the fibrosis veneers was between 6 and 7% and the initial temperature was about 25 °C. The average speed of oven increasing temperature was about 2 °C/min from initial temperature to the required temperature, but the temperature increasing rate could not be controlled constantly. After 6 h of insulation, the temperature of oven declined steadily with a speed of about 3 °C/min to 30 °C.

Color measurement

The CIE Lab and LhC systems were adopted to evaluate the color changes of poplar samples after the heat treatment. The CIE Lab system was characterized by three parameters L^*, a^* and b^* ($L^* = 100$ for pure white, $L^* = 0$ for total black; $+a^*$ for red, $-a^*$ for green; $+b^*$ for yellow, $-b^*$ for blue), meanwhile, the parameters h and C were the representative of the LhC system where C represented for color saturation and h represented for tone (h and C can be calculated by a^* and b^*). The color was measured with a colorimeter called CM-3600d (Minolta, Tokyo, Japan), operating at 360–740 nm with a measuring head of 8 mm in diameter, CIE Illuminant D 65, and observation angle of 10°. The total color difference (ΔE) was calculated by the following equation:

$$\Delta L^* = L^* - L_0^* \tag{1}$$

$$\Delta a^* = a^* - a_0^* \tag{2}$$

$$\Delta b^* = b^* - b_0^* \tag{3}$$

$$\Delta E^* = [(\Delta L^*)^2 + (\Delta a^*)^2 + (\Delta b^*)^2]^{1/2} \tag{4}$$

$$h = \arctan(b^*/a^*)180°/\pi \tag{5}$$

$$C = (a^{*2} + b^{*2})^{1/2}. \tag{6}$$

The data of reflection spectra of poplar samples could also be obtained through the measure process. In addition, the reflectance spectrum would be converted to the K–M function through the following expression [21].

$$F(\gamma_\lambda) = \frac{K}{S} = \frac{(1 - \gamma_\lambda)^2}{2\gamma_\lambda} \tag{7}$$

$$\gamma_\lambda = \frac{\gamma_{(sample)}}{\gamma_{(standard)}} \tag{8}$$

K and S were the absorption and scattering coefficient, respectively, and γ_λ was the reflectance ratio between poplar samples and a Whatman cellulose paper (no. 42) with a defined porosity. Where $\gamma_{(sample)}$ was the poplar sample reflectance and $\gamma_{(standard)}$ was the reflectance of a cellulose paper (Whatman paper no 42.).

Holocellulose analysis

The veneers for each treatment were selected randomly and milled to get powders (0.3–0.4 mm), which was separated by sieving. The dust was stored and utilized for further chemical analyses.

With regard to holocellulose contents analysis, GB/T 2677.10-1995 [22] was available. A test to determine holocellulose contents was carried out on the basis of the standard. The essence of the method was to remove the lignin by treating the samples with sodium chlorite when the pH is 4–5. First, 2 g (accurate to 0.0001 g) of powders was extracted by benzene–ethanol, and then were placed in 65 mL distilled water, which was heated to 75 °C. Acetic acid (0.5 mL) and sodium chlorite (0.6 g) were added into the solution each hour until the powders turned white. The mixture was then filtered and washed by shaking with distilled water until the filtrate was no longer acidic, washed with acetone three times, and dried at 105 ± 2 °C until a constant mass was achieved. Two sets were prepared for each sample, and the error rate of calculation of the two measurements was determined to be less than 0.4%. The results presented are the average of two sets of tests.

α-Cellulose analysis

As regards α-cellulose contents analysis, GB/T 744–1989 [23] was available. A test to determine α-cellulose contents was carried out on the basis of the standard. The holocellulose (separated according to the description above) was infused with 17.5% NaOH (30 mL) then placed in a water bath (20 °C) for 45 min. A total of 30 mL of distilled water was then added. Next, the mixture was filtrated and washed with 9.5% NaOH (25 mL) three times, and washed again

with distilled water (400 mL). Acetic acid was then added to the residue and was held for 5 min. The residue was washed with distilled water until the filtrate solution was no longer acidic, and dried at 105 °C until a constant mass was achieved. Two sets for each sample were prepared, and the error rate of calculation of the two measurements was less than 0.4%. The result presented was the average of two sets.

Acid-insoluble lignin analysis

With respect to acid-insoluble lignin contents analysis, GB/T 2677.8-1994 [24] was available. A test to determine acid-insoluble lignin contents was carried out on the basis of the standard. First, a total of 1 g (accurate to 0.0001 g) of powders was extracted by benzene–ethanol. The samples were hydrolyzed with 15 mL of 72% H_2SO_4 at 15 °C and then placed in a water bath at 20 °C for 2.5 h. Second, samples were diluted to 3% H_2SO_4 and then boiled at 100 °C for 4 h. After the second cycle of hydrolysis, lignin was filtered, washed with distilled water until the filtrate was no longer acidic, and then dried at 105 ± 2 °C until a constant mass was achieved. Two sets for each sample were prepared, and the error rate of calculation of the two measurements was determined to be less than 0.4%. The results presented are the average of two sets of tests.

Extractives analysis

Several tests to determine the contents of hot water extractives, cold water extractives, benzene–alcohol extractives and 1%NaOH extractives were carried out according to the standard GB/T 2677.4-1993 [25], GB/T 2677.5-1993 [26] and GB/T 2677.6-1993 [27], respectively. Extractives were calculated as a percentage of the extracted oven-dry weight of the sample. Each sample was analyzed twice.

Surface analysis of samples by X-ray photoelectron spectroscopy

The elemental and chemical data of different poplar samples heat treated or untreated were provided by an axis-ultra X-ray photoelectron spectrometer from the Analytical Instrumentation Center of Beijing University. The poplar raw wood, untreated fibrosis veneers, fibrosis veneers treated at 160 °C/0.3 MPa for 2 h and fibrosis veneers treated at 180 °C/0.3 MPa for 2 h samples were prepared with a size of approximately 4 mm $(L) \times 4$ mm $(R) \times 1$ mm (T). Three samples for each of four conditions were measured by XPS analysis. All the samples were protected from pollution source before testing. An aluminium monochromatic source with a power of 300 W potential were used to record the spectra. Similarly, a nominal energy resolution of 0.48 eV for Ag 3d 5/2 was utilized to obtain the high resolution spectra,

and then the binding energies of survey scans range from 1100 to 0 eV, which were used for chemical analysis. The pass energy of 20 eV with a step size of 0.1 eV was used to record the survey spectra-quantitative elemental analyses of untreated and heat-treated samples. Casa XPS and origin software were utilized to process data.

Gas chromatography–mass spectrometry analysis

The untreated fibrosis veneers and fibrosis veneers treated at 180 °C/0.3 MPa were cut into small pieces, weighted 3 g and soaked in a mixture solution of benzene and ethanol (2:1) for 24 h at room temperature. The extraction solution was evaporated and detected by a GC–MS (Agilent 7890 A, Agilent, California) with a chromatographic column called RTX-17MS (30 m $\times$ 0.25 mm $\times$ 0.25 μm). The column temperature was programmed as follows: rose to 50 °C and maintained 1 min, a speed of 5 °C/min to 240 °C and keep 1 min, and then, a speed of 10 °C/min to 280 °C and keep 10 min. In addition, helium was used as a carrier gas at a flow rate of 1 mL/min. The experimental process adopt splitless injection mode with a split ratio of 30:1 and inhalation of 1 mL sample. The MS part was executed as the following parameters: electron multiplier (EM) voltage of 1306 V, MS source at 230 °C, and MS quad at 150 °C. The individual peaks calculated by peak area were compared with the Wiley computer mass library. The relative percentage of each peak area was calculated using the normalization method. Furthermore, chemical composition was identified by NIST library (established by the US National Institute of Standards and Technology) [28].

Chemical structure analysis by solid-state NMR

Solid-state ^{13}C NMR spectra of the untreated and treated fibrosis veneer samples were acquired at room temperature with a BRUKER AV400 NMR spectrometer (Bruker Corporation, Germany), operating magic angle sample spinning (MAS) rates of 4 and 8 kHz a proton frequency of 100.7 MHz. The Bruker cross-polarization (CP) MAS probe head was 7 mm Bruker. In addition, the combination of CPMAS and high-power proton decoupling methods were used. Samples were packed in MAS 4-mm-diameter zirconia rotors. The chemical shift values were calibrated indirectly with the glycine carbonyl signal set to 176.03 ppm relative to tetramethylsilane. All the spectra were run for 1800 scans. All the integrals were corrected by a factor taking into account the dynamics of the ^{13}C magnetisation to obtain quantitative data from the CPMAS experiments. The integrals were normalized by filling the rotors with the samples and the loss of mass was related to the lower of signal induced by the thermal treatment. If the heat-treatment affected one of the wood components intensely,

the proportion of sample weight of the other components automatically increases, although they may also have been affected to some extent. Thus, the peak area divided by the initial mass of raw wood remains constant as long as the structure of the considered atom is unchanged and this value decreases when the treatment has induced structural modifications. As a result, comparing CPMAS spectra recorded under identical conditions and acquiring semi-quantitative information could be realized. Wood NMR spectra was decomposed using DIMFIT software on account of signal overlapping [29]. Based on the signal assignment, the NMR spectrum of untreated fibrosis veneers was first fitted. The NMR-signal parameters (linewidth, chemical shift) were then used as input data to decompose the NMR spectra of heat-treated fibrosis veneer samples.

To summarize, the normalized areas were obtained by:

"normalised peak areas" $=$ peak area $x(1 - \Delta m)/m_{rotor}$,

where Δm is the relative mass loss of the sample during heat treatment and m_{rotor} is the sample weight (in the NMR rotor).

Results and discussion

Surface discoloration

As was shown in Fig. 2, the color of the poplar samples changed markedly before and after the treatment, as expected. The color of poplar, untreated fibrosis veneer, fibrosis veneers treated at 160 °C/0.3 MPa and 180 °C/0.3 MPa for 2 h was, respectively, light white, yellowish brown, yellow brown and dark chocolate.

Figure 3 showed that from a–d the surface brightness L^* and tone h decreased, as a result of which, the fibrosis
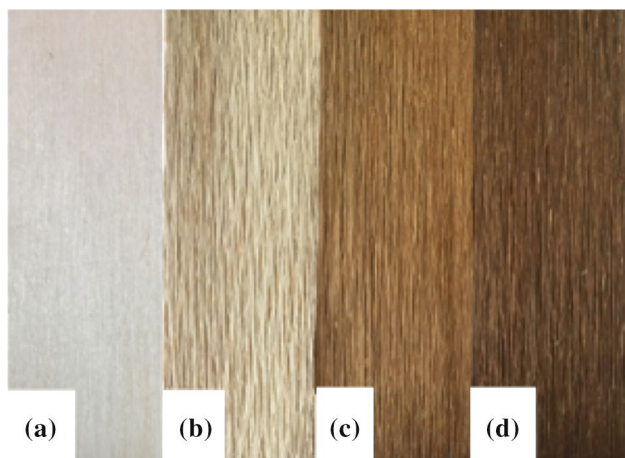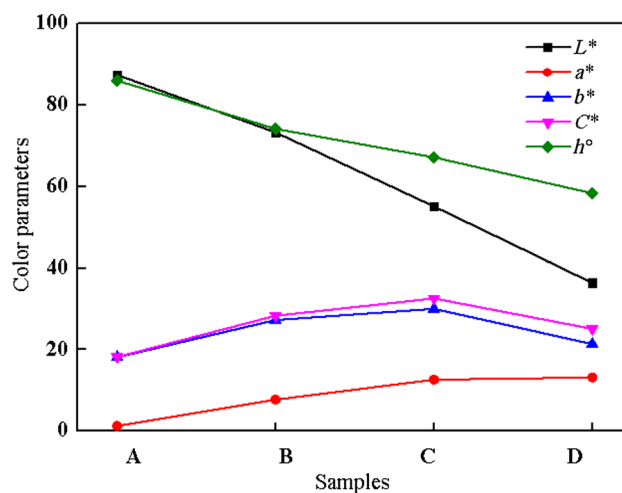
Fig. 3 Surface color parameters change of poplar fibrosis veneer with three conditions. A Poplar. B Untreated fibrosis veneer. C Heat-treated fibrosis veneer (160 °C/0.3 MPa). D Heat-treated fibrosis veneer (180 °C/0.3 MPa)

veneer heat-treated under the condition of 180 °C/0.3 MPa was the darkest. The reason why the parameters L^* and h of b was lower than a was that the poplar veneer was squeezed by the special machinery to obtain fibrosis veneers, and then the extracts moved to the surface. While it also can be seen that parameters a^*, b^* and C increased simultaneously. The phenomenon indicated a red–yellow development. One explanation why there was a substantial change of the color after heat treatment, was that the lignin in acidic conditions caused by heat treatment lead to more phenolic hydroxyl groups, and newphenolic hydroxyl groups formation, and then the color of the samples was deepened [20]. The color of wood is determined by lignin and extractive, which contains carboxyl, unsaturated double bond, conjugated chromophores and an auxochrome group [30]. Generally, the color reflects the relative contents of basic chemical components in wood. The degradation of the polysaccharides caused by heat treatment lead to an increase in the relative contents of lignin and extractive. As a result, wood surface color changes. On the other hand, extractives that moved with vapor from the interior to the wood surface deepen the surface color of wood [31].

Figures 4 and 5 showed the reflectance spectra and K–M curve of poplar samples. In the range of 400–700 nm, all the reflectance spectra curves raised and K–M curves declined. According to the relationship between color and wavelength, the wood reflected much more the red–yellow part of the light, which formed the warm color tone of the wood. From A to D, the rises of K–M curve may be associated the formation of biphenyl, conjugated, and C=O structures after the heat treatment [32, 33].

Fig. 2 Surface color of poplar fibrosis veneer with three conditions. **a** Poplar. **b** Untreated fibrosis veneer. **c** Heat-treated fibrosis veneer (160 °C/0.3 MPa). **d** Heat-treated fibrosis veneer (180 °C/0.3 MPa)
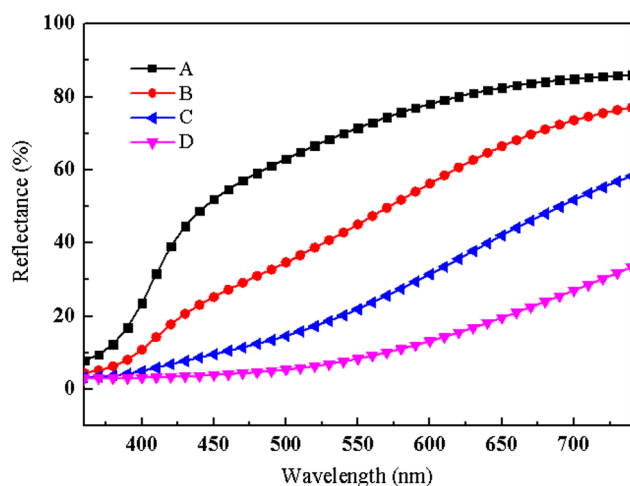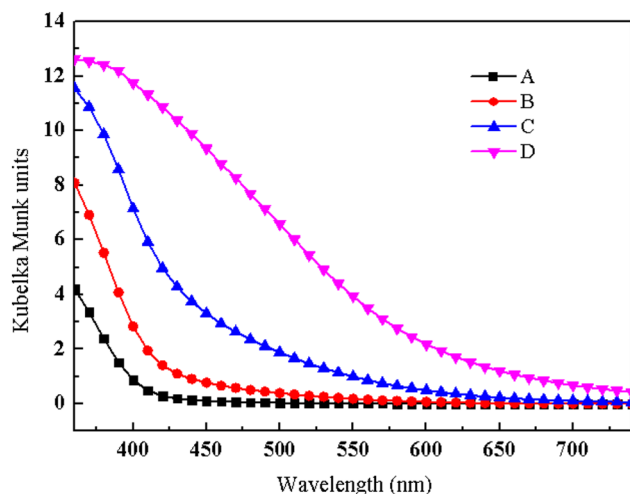
Fig. 4 Reflection spectra of Poplar samples. A poplar. B Untreated fibrosis veneer. C Heat-treated fibrosis veneer (160 °C/0.3 MPa). D Heat-treated fibrosis veneer (180 °C/0.3 MPa)

Fig. 5 Evolution of *K–M* spectra of poplar samples. A Poplar. B Untreated fibrosis veneer. C Heat-treated fibrosis veneer (160 °C/0.3 MPa). D Heat-treated fibrosis veneer (180 °C/0.3 MPa)

## Changes in contents of chemical components and extractives

Table 1 demonstrated that chemical reactions of the chemical components had taken place during the heat treatment, which resulted in changes in the contents of holocellulose, α-cellulose, lignin, and extractives. There was a downward trend in the contents of holocellulose and α-cellulose after heat treatment, whereas the contents of lignin and extractive (cold water, hot water, benzene–alcohol, NaOH) showed the opposite trend. The most conspicuous change was for hemicellulose content, which decreased by nearly 10.27 and 35.54% at heat treatment temperatures of 160 °C/0.3 MPa and 180 °C/0.3 MPa, respectively. These results were highly consistent with those reported in previous studies [34–37]. The hemicellulose was considerably more susceptible to thermal degradation than other wood components due to its branched structure and amorphous tissues. The degradation products of hemicellulose were mostly small-molecule saccharides, such as galactose, xylose, mannose and so on [38]. The content of lignin in fibrosis veneers increased during the heat treatment was partly due to the loss of polysaccharide, which gave rise to the increase of relative proportion of the lignin. Owing to the degradation of chemical components, the content of extractives available increased [39, 40].

XPS analysis

XPS analysis is one of the most effective and sensitive techniques to analyze wood surface chemical compositions and valence state of elements, which can be used to explain heat treatment mechanism. Wood contains approximately 42–50% cellulose, 25–30% hemicellulose, 20–25% lignin and 5–8% extractives [41]. The elemental composition of these compounds mainly includes carbon (C), hydrogen (H) and oxygen (O). All the elements of wood which are analyzed to a depth of about 10 nm are detectable by the XPS analyses except hydrogen atoms. The typical XPS survey spectra of poplar raw wood, untreated poplar fibrosis veneers and heat-treated fibrosis veneers samples were illustrated in Fig. 6. According to the graph, the peaks of carbon and oxygen representative the major elements of the sample present at around 286 and 532 eV. That was highly consistent with

Table 1 Changes in the contents of chemical components and extractives of the fibrosis veneer samples

Sample	Holocellu-lose (%)	α-Cellulose (%)	Hemicellu-lose (%)	Lignin (%)	Extractives (%)			
					Cold water	Hot water	Benzene–alcohol	NaOH
Control	62.85	41.52	21.33	26.25	2.07	5.93	4.97	19.20
160 °C/0.3 MPa	59.77	40.63	19.14	28.67	3.07	6.21	5.09	21.19
180 °C/0.3 MPa	53.33	39.58	13.75	33.61	3.28	6.63	5.82	24.14
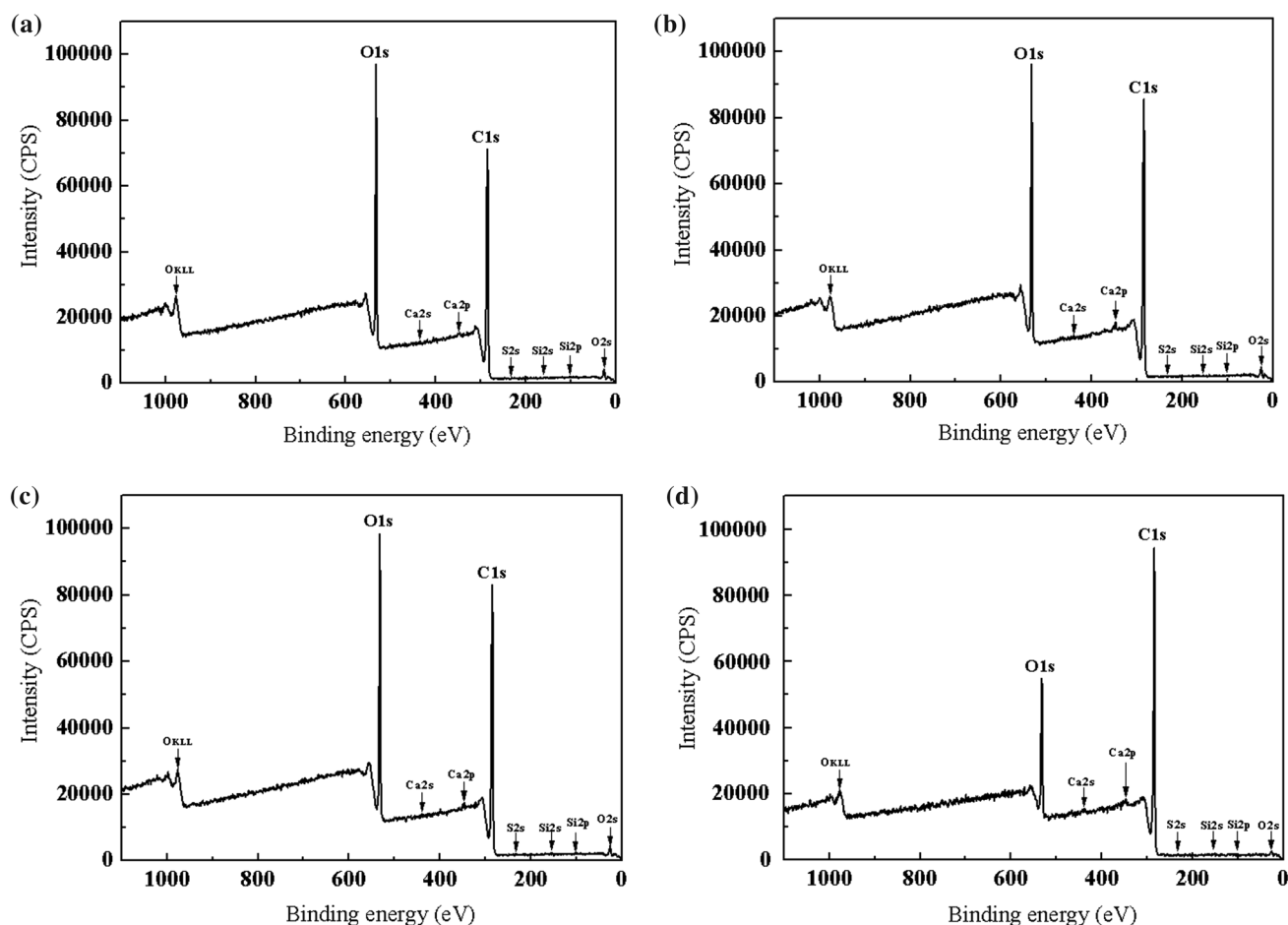
Fig. 6 XPS survey spectra of different poplar samples. **a** Poplar raw wood. **b** Untreated poplar fibrosis veneers. **c** Heat-treated fibrosis veneer (160 °C/0.3 MPa). **d** Heat-treated fibrosis veneer (180 °C/0.3 MPa)

previous studies for woody materials [16, 42]. Furthermore, a small amount of calcium (Ca), silicon (Si) and sulfur (S) also were detected on the surfaces of the samples by XPS at corresponding emission peaks.

The high-resolution C1s XPS spectra of the four samples were treated through peak-spilt processing to obtain a deeper insight into the surface chemical structures modification, which indicated the presence of four peaks of carbon atoms for untreated and heat-treated samples (seen Table 2; Fig. 7). The C1s spectra were composed of several subunits in which C–C, C–H, C–O, C=O, O–C–O and O=C–O linkages could be classified. Most of the C1 carbon, which linked to carbon (C–C) or hydrogen (C–H) groups, could be attributed to aliphatic and aromatic carbons of lignin and extractives. The C2 carbon bonded with one oxygen atom (C–O) mainly derives from cellulose and hemicelluloses. The C3 carbon bonded to a carbonyl or two non-carbonyl oxygen atoms (C=O, O–C–O) corresponds to hemicelluloses and cellulose. Similarly, the C4 (O–C=O) carbon bonded to a carbonyl and a non-carbonyl

oxygen atom was associated with hemicelluloses and extracts [43, 44]. As was listed in Table 2 and Fig. 4 that the C1 carbon atom had a lower binding energy of about 284.8 eV. Compared with the binding energy of C1, the C2 carbon increased slightly to 286.5 eV. The C3 carbon appeared at a higher binding energy of 288.0 eV, while the C4 was pointed out at a binding energy of 289.2 eV. That was in agreement with the previous researches [45]. The results showed that C1 carbon and C2 carbon constitute approximately 90% of all the carbon on the surfaces of the four samples, whereas C3 carbon and C4 carbon were in minority. After heat treatment, the percentage of the C2 component declined from 41.48 to 11.51%, whereas that of C1 increases from 48.38 to 77.26%. The contributions of C3 were found to be a slight decline during heating, while those of C4 tend to be the opposite direction. It also can be concluded that C1 (C–C, C–H) was the most important contributions to all samples surfaces. All the data indicated that the samples surfaces become poorer in carbohydrate after heating, owing to the fact that

Table 2 C1s and O1s peak of different poplar samples

Element constitution	Binding type	Binding energy/eV	Untreated	Fibrosis veneers	160 °C/0.3 MPa	180 °C/0.3 MPa
C/%	–	–	74.26	75.82	76.91	83.15
O/%	–	–	24.92	23.15	22.45	16.01
O/C	–	–	0.34	0.31	0.29	0.19
C1/%	C–C or C–H	284.8	48.38	52.37	57.04	77.26
C2/%	C–O	286.5	41.48	37.74	33.26	11.51
C3/%	O–C–O or C=O	288.0	8.11	7.89	7.20	5.33
C4/%	O–C=O	289.2	2.03	2.00	2.50	5.90
C1/C2	–	–	1.17	1.39	1.71	6.71
C_{OX}/C_{UNOX}	–	–	1.07	0.91	0.75	0.29
O1/%	O–C=O	532.2	4.53	4.92	5.79	6.46
O2/%	C–O–, C=O, C–O–C, O–C=O	534.35	95.47	95.08	94.21	93.54
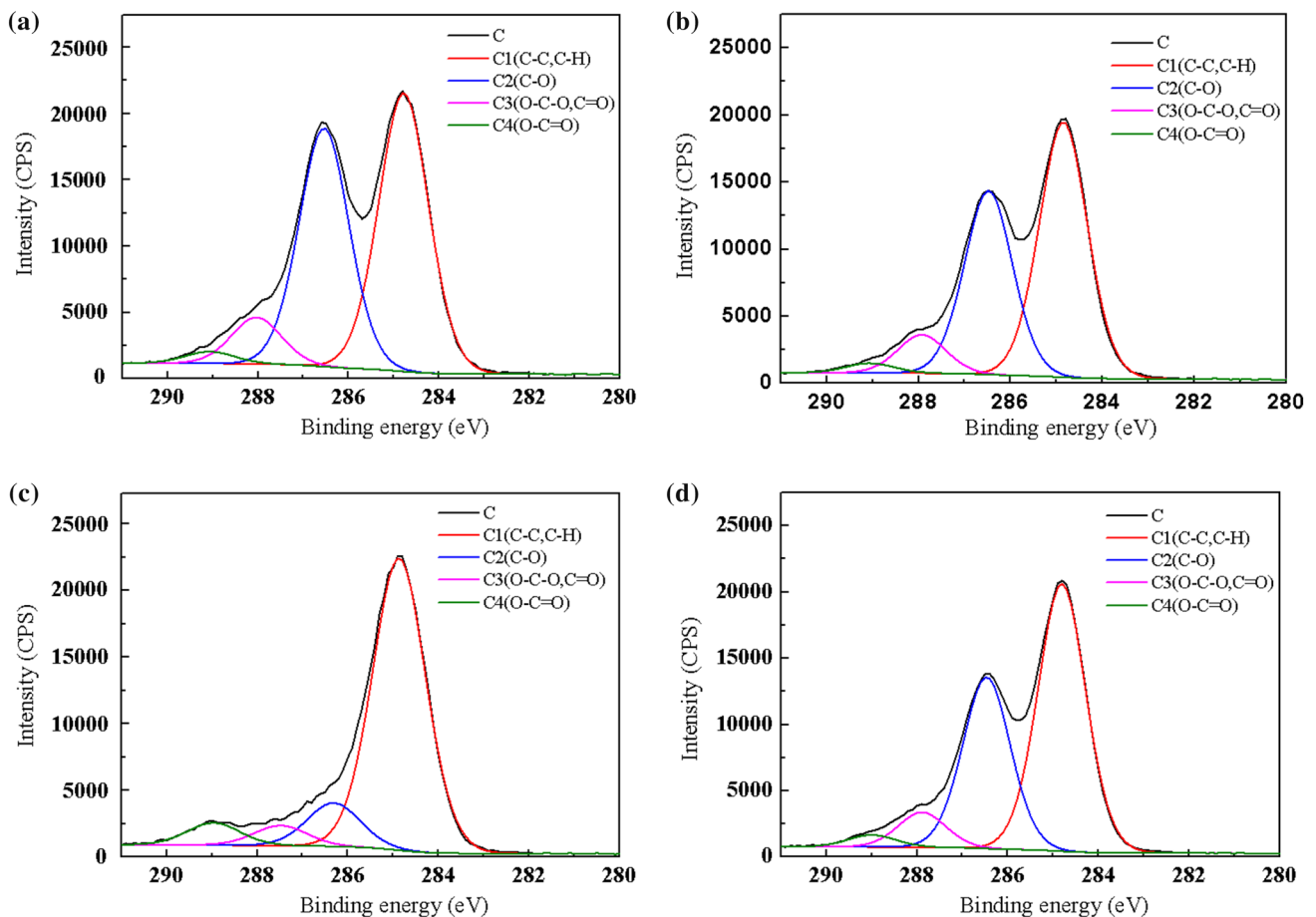
Fig. 7 C1s XPS survey spectra of different poplar samples. **a** Poplar raw wood. **b** Untreated poplar fibrosis veneers. **c** Heat-treated fibrosis veneer (160 °C/0.3 MPa). **d** Heat-treated fibrosis veneer (180 °C/0.3 MPa)

hemicelluloses and cellulose were highly sensitive to high temperature and degrading during the heat treatment process. In contrast, the results confirmed that the relative contents of lignin on the surfaces increased after heating.

Those finding of XPS verified the results of the contents of chemical components analysis.

The O1s spectrum could be divided into two parts according to the state of oxygen (seen Fig. 8; Table 2). The O1
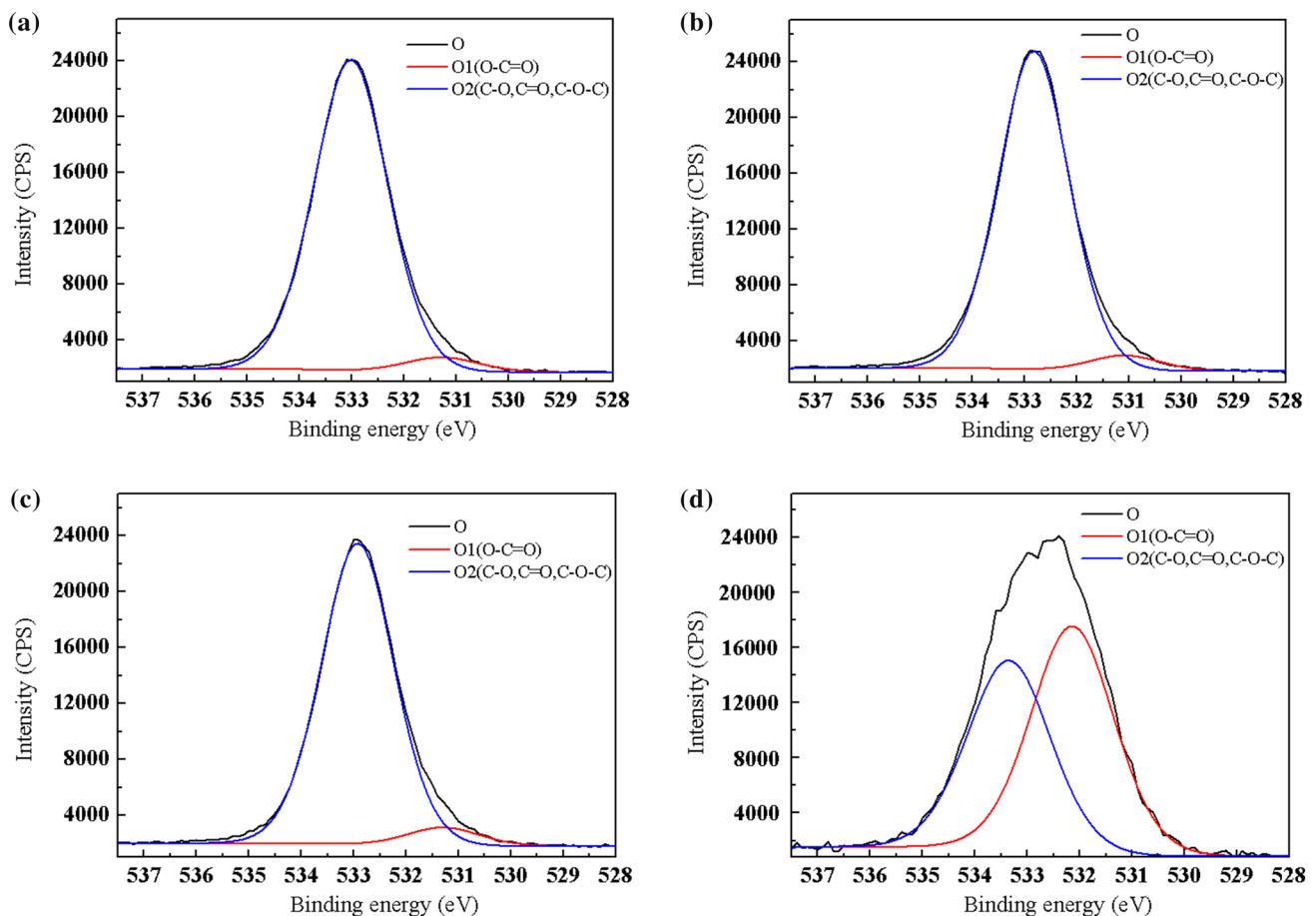
Fig. 8 O1s XPS survey spectra of different poplar samples. **a** Poplar raw wood. **b** Untreated poplar fibrosis veneers. **c** Heat-treated fibrosis veneer (160 °C/0.3 MPa). **d** Heat-treated fibrosis veneer (180 °C/0.3 MPa)

peak corresponded to oxygen atoms bonded to carbon with a double bond (O–C=O), while the O2 peak originated from oxygen bonded to carbon with a single bond (C–O–). The O1 peak could be distinguished from the O2 peak in that the figure of binding energy of the O1 peak was a little lower than that of the O2 peak. The O1 component had been deduced to be associated with lignin and extractives in wood material. The O2 component, however, was considerably associated with hemicelluloses and cellulose [46, 47]. Therefore, the contents of the O1 component and the O2 component fluctuations after treatment were indications of chemical composition transformation. According to Table 2 and Fig. 8 presented, the O1 components slightly increased and the O2 component decreased after heat treatment, which indicated that the sample surfaces became poorer in carbohydrate content and richer in the lignin and extractive content. This finding agreed with chemical components analysis results.

According to the literature [48], cellulose including five carbon atoms of C2 and one of C3 had the O/C ratio of 0.83. Correspondingly, hemicelluloses, which were

constituted of fewer than five carbon atoms of C2 and one atom of C3, possessed an O/C of approximately 0.8. As far as lignin was concerned, the C1 and C2 classes comprised a high proportion in its structure, the theoretical value of O/C of which was roughly 0.33. The extractives had the lowest O/C ratio of 0.1, owing to the fact that they mainly included lipophilic compounds, such as triglycerides, fatty acids, and sterols [49]. Therefore, calculating the theoretical O/C ratio was feasible to evaluate the degradation degree of cellulosic materials and polymers when XPS was applied to characterize material surfaces. The high content of the polysaccharides in the wood surface brought about a high O/C ratio. Conversely, a low ratio was caused by more lignin and extractives on wood surfaces. The results of O/C ratio for untreated poplar, poplar fibrosis veneers and heat-treated fibrosis veneer samples were presented in Table 2. There was a slightly downward trend in the ratio of the oxygen to the carbon as the processing conditions change suggesting a modification of surface composition of the wood. The fact samples taken on the surface of poplar fibrosis veneers present relative lower O/C ratio to those taken from untreated
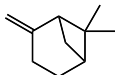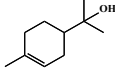
poplar may be due to the significant contamination of the surface by the extractives. The poplar fibrosis veneers are produced by mechanical extrusion, as a consequence of which, a fairly large amount of the extractives migrated to the surface from within the wood structure. It was also observed that O/C ratio declines after heat treatment of poplar samples and fell markedly with heat treatment temperature increasing, which is in agreement with the previous researches [42, 50]. One explanation why the O/C ratio declined is that hemicellulose degradation. This is in agreement with the chemical component analysis of heat-treated wood where the content of hemicellulose dropped sharply

and then the relative content of lignin increased. Moreover, it is important to note that the formation of volatile due to thermal degradation and evaporation of volatile extractives should reduce oxygen contents.

GC–MS analysis

From Table 3 and Fig. 9, we could see that untreated fibrosis veneers contained a lot of carboxylic acid, mainly for the oxalic acid. By contrast, Fig. 10 identified more and relative high contents of extractives. Most of the extractives were generated from hemicelluloses degradation (seen Table 4).

Table 3 Main composition of benzene and ethanol extraction from the untreated fibrosis veneers

Peak	CAS	English name	Relative percent (%)	Structural formula
1	144-62-7	Oxalic acid	35.7	
2	141-46-8	Acetaldehyde	25.51	
3	000127-91-3	beta-Pinene	12.4	
4	001632-73-1	Bicyclo[2.2.1]heptan-2-ol, 1,3,3-trimethyl-	8.5	
5	000098-55-5	3-Cyclohexene-1-methanol, alpha,alpha.4-trimethyl-	14.7	

Every chemical compound has it's own number assigned by Chemical Abstracts Service (CAS)

Fig. 9 GC–MS chromatogram of benzene and ethanol extraction from the untreated fibrosis veneers
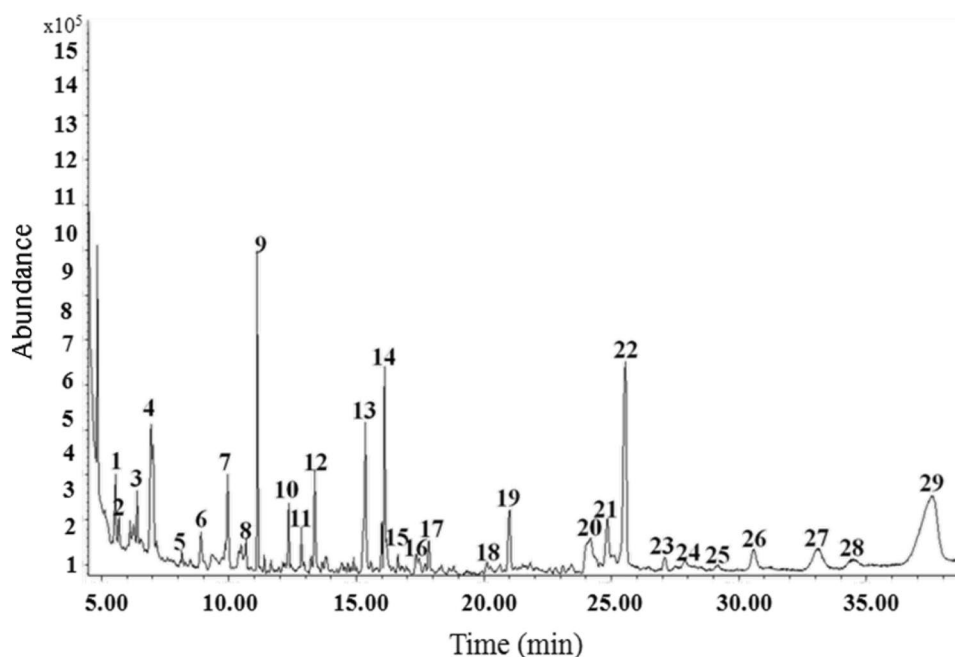
The degradation product phenols were derived from degradation of hemicelluloses and cellulose during the thermal treatment, and could be classified into 4 categories: aldehydes, ketones, monomeric sugars and alkanes. The relative percent of propanoic acid, 2,2-diethoxy-, ethyl ester, 2,4-decadienal, furan, ethenyl-, 2,4-decadienal, methylnaphthalene, 3-octen-2-one, and furfural were much higher for fibrosis veneers treated at 180 °C/0.3 MPa. In the early stages of decomposition of hemicellulose, ketones and aldehydes emerged owing to the structure fracture of 4-o-methyl D-glucuronic acid. In addition, the furan derived from 4-o-methyl D-glucuronic acid of the link fracture of xylan [51].
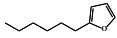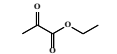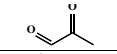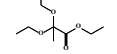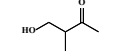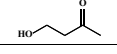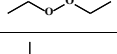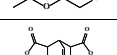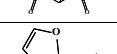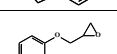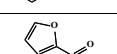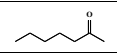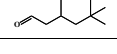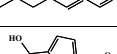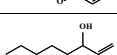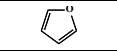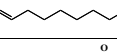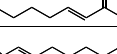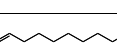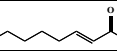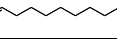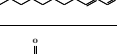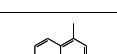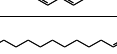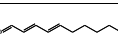
NMR analysis

Lignin, cellulose and hemicelluloses containing different carbons were the main components of wood, and their primary structure had been illustrated in Fig. 11 [14]. Resonance assignment of ^{13}C NMR signals of raw wood had been studied widely over the last decades, the unanimous conclusions of that were summarized in Table 5. With respect to hemicelluloses, the focus was set on resonances resulting from related carbon atoms. At 172 ppm, the signal #1 was assigned to the –COO– carbons of the hemicelluloses acetoxy groups. Similarly, the signal #16 at 21 ppm was assigned to the CH_3– carbons of the hemicelluloses acetyl units. In addition, the signal #8′ with a wide and weak peak, which was near the signal #8, was generated by the C-1 of hemicelluloses. Owing to amorphous structure of hemicelluloses, the shoulder of the signal #8′ was explicably wide.

For cellulose, the following signals and carbon atoms were concerned. The peaks of large signal (#8–#14) occurring in the region between 60 and 105 ppm were specific of carbons from cellulose and hemicelluloses carbohydrates [52–55]. These peaks were predominantly attributed to cellulose, the remaining part to hemicelluloses carbohydrates. The peak signed #8 occurring at 104.8 ppm was considerably intense. This signal was assigned to the C-1 of cellulose in spite of some inevitable overlap with aromatic carbons of hemicelluloses. The signals #9 at 88.7 ppm and #10 at 83.8 ppm were both corresponding to the C-4 of cellulose allomorphs (ordered and disordered/amorphous cellulose). Particularly, the signal #9 standed for disordered/amorphous cellulose at the surface of crystalline microfibers, conversely, the signal #10 was indicative of crystalline cellulose. In the same way, for lignins, the following signals and carbons were used to analyze the modifications of structure of the lignin. The peaks caused by carbons from aromatic units of lignin appeared in the region between 105 and 160 ppm. At 152.6 ppm, the signal #2 was classically due to C-3 and C-5 of syringyl units in etherified that involved in β–O–4 structures. The signal #3 contains contribution not only C-3 and C-5 of syringyls in non-etherified structures but also C-3 and C-4 of guaiacyls in etherified and nonetherified structures. In particular, the shoulder #15 at 55.7 ppm was mainly assigned to resonance of carbon atoms of methoxyl groups occurring in aromatic units.

The qualitative analyses of the main signals of NMR spectra were carried out in this study. It was worth mentioning that spectrum A was typically representative of ^{13}C CPMAS spectrum of untreated fibrosis veneers in

Table 4 Main composition of benzene and ethanol extraction from fibrosis veneers treated at 180 °C/0.3 MPa

Peak	CAS	English name	Relative percent (%)	Structural formula
1	003777-70-6	Furan, 2-hexyl-	2.12	
2	617-35-6	Ethyl pyruvate	0.65	
3	78-98-8	Methylglyoxal	1.57	
4	7476-20-2	Propanoic acid,2,2-diethoxy-, ethyl ester	4.17	
5	3393-64-4	2-Butanone,4-hydroxy-3-methyl-	0.97	
6	590-90-9	2-Butanone, 4-hydroxy-	2.1	
7	628-37-5	Peroxide, diethyl	2.45	
8	109-59-1	Ethanol,2-(1-methylethoxy)-	4.6	
9	1719-83-1	Bicyclo[2.2.2]oct-7-ene-2,3,5,6-tetracarboxylic acid dianhydride	5.54	
10	31093-57-9	Furan, ethenyl-	2.32	
11	122-60-1	Glycidyl phenyl ether	1.55	
12	98-01-1	Furfural	3.32	
13	110-43-0	2-Heptanone	4.72	
14	5435-64-3	3,5,5-trimethyl-Hexanal	5.35	
15	2463-63-0	2-Heptenal	1.06	
16	67-47-0	5-Hydroxymethylfurfural	1.07	
17	3391-86-4	1-Octen-3-ol	1.54	
18	110-00-9	Furan	1.11	
19	124-13-0	octanal	2.68	
20	1669-44-9	3-Octen-2-one	4.32	
21	2463-53-8	2-Nonenal	3.45	
22	124-19-6	1-Nonanal	6.35	
23	14309-57-0	3-Nonen-2-one	0.47	
24	112-31-2	Decanal	0.55	
25	2463-77-6	2-Undecenal	0.76	
26	14476-37-0	4-Undecanone	1.47	
27	1321-94-4	methyl-Naphthalene	4.17	
28	112-44-7	Undecanal	2.54	
29	2363-88-4	2,4-Decadienal	10.34	

Every chemical compound has it's own number assigned by Chemical Abstracts Service (CAS)

Fig. 11 Schematic representation of the main components of wood: **a** cellulose, **b** xylan (main component of hemicelluloses), **c** lignin. Hemicelluloses acetyl groups (–OOC–CH₃) are not shown in **b** since the *O*-acetyl substitution can occur at any of the hydroxyl position in xylan. **c** Corresponds to a syringyl dimer. Replacement of the methoxyl groups –OCH₃ given in parenthesis by a hydrogen atom leads to the guaiacyl structure
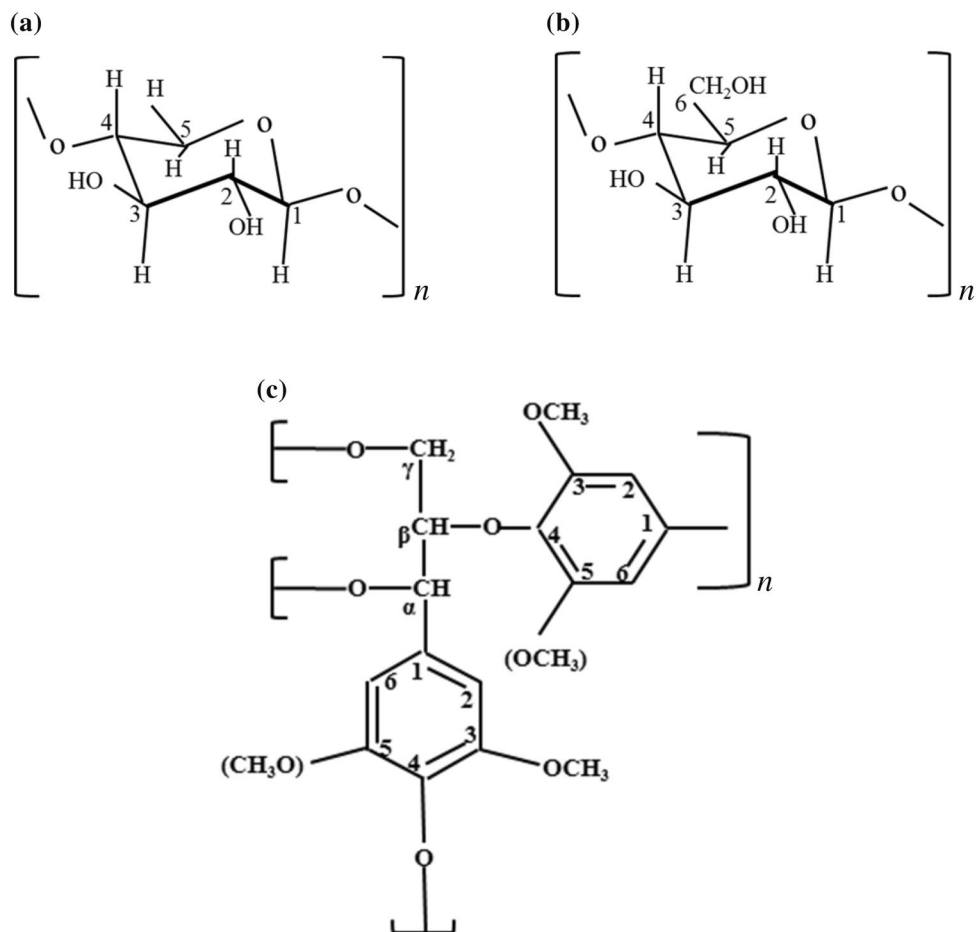
Table 5 Resonance assignment of ^{13}C NMR spectrum of raw wood

Resonance number	Chemical shift (ppm)	Assignments
1	172	Hemicelluloses: –$\underline{C}$OO–R, CH₃–$\underline{C}$OO–
2	152.6	Lignins: S-3(e), S-5(e)
3	148–147	Lignins: S-3(ne), S-5(ne), G-3(ne,e), G-4(ne,e)
4	138.5–138	Lignins: S-1(e), S-4(e), G-1(e)
5	134–133	Lignins: S-1(ne), S-4(ne), G-1(ne)
6	121	Lignin: G-6
7	114–106	Lignins: S-2, S-6, G-5, G-6
8	104.8	Cellulose: C-1
8′	104–101	Hemicellulose: C-1
9	88.7	Carbohydrates: C-4 cellulose (ordered)
10	83.8	Lignins: C$_\beta$, Carbohydrates: C-4 cellulose (disordered)
11	74.8	Lignin: C$_\alpha$, Carbohydrates: C-2, -3, -5
12	72.2	Carbohydrates: C-2, -3, -5
13	64.7	Carbohydrates: C-6 cellulose (ordered)
14	61.6	Lignins: C$_\gamma$, Carbohydrates: C-6 cellulose (disordered)
15	55.7	Lignin: O$\underline{C}$H₃
16	21	Hemicellulose: $\underline{C}$H₃–COO–

NMR nuclear magnetic resonance, *S* carbon in syringyls (aromatic unit with two methoxyl groups), *G* carbon in guaiacyls (aromatic unit with only one methoxyl), *ne* in non-etherified arylglycerol β-aryl ethers, *e* in etherified arylglycerol β-aryl ethers
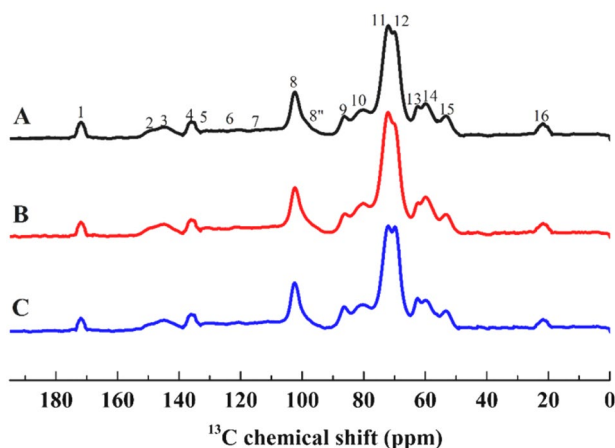
Fig. 12 50 MHz ^{13}C CPMAS high-resolution solid-state NMR spectra of raw and heat-treated samples of poplar wood. A untreated fibrosis veneers (dried at 60 °C), B heat-treated fibrosis veneer (160 °C/0.3 MPa), C heat-treated fibrosis veneer (180 °C/0.3 MPa). In spectrum A, the peaks are numbered from 1 to 16 and the corresponding assignment can be found in Table 3

Fig. 12, which illustrated the spectra of samples of fibrosis veneers treated under different conditions. Since cellulose C-1 (signal #8 at 104.8 ppm) was insensitive to thermal treatment below 245 °C, we could utilize the intensity of the signal of cellulose C-1 to normalize the other signals [14]. That was an effective method to better highlight the transformations brought about by the thermal treatment. The spectra A could be distinguished from B and C, owing to the fact that qualitative changes with respect to intensity of signals can be evidenced only after a very close inspection. The ^{13}C NMR signal integrals of signals #1 and #16 at 172 and 21 ppm assigned to hemicelluloses acetyls groups (–COO– and CH$_3$–), respectively, decreased as the temperature increased. The degradation of hemicelluloses was also clearly demonstrated by the unambiguous vanishes of signal #8″ assigned to hemicelluloses C-1. All the features of hemicelluloses showed that it was sensitive to heat treatment. The results were highly consistent with previous studies of XPS and chemical component analysis. The evolution of signals #2 and #3 assigned to syringyl C-3 and C-5 in β–O–4 structures(etherified and in non-etherified, respectively) could be observed clearly. One explanation why there was a slight decrease of resonance #2 at 180 °C/0.3 MPa was that lignins depolymerized by cleavage of the β–O–4 bonds or syringyls demethylated. The intensity of signal #15 assigned to methoxyl groups fell markedly at 180 °C/0.3 MPa, which could explain the decrease of resonance #2 to a great extent. The signals #4 and #5 were assigned to both syringyls and guaiacyls included in β–O–4 bonds. Considering that the variation of the signal #4 could not be observed at 160 °C/0.3 MPa, it was concluded that the cleavage of β–O–4 bonds had not taken place noticeably at
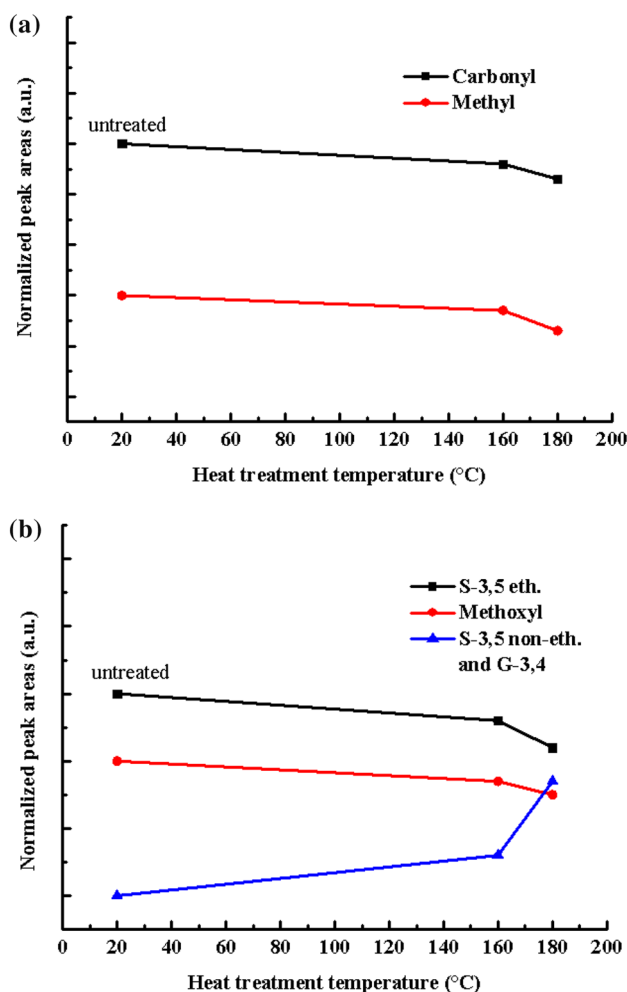
Fig. 13 Evolution of different ^{13}C NMR signal integrals as a function of the torrefaction temperature: **a** hemicelluloses signals #1 (carbonyl) and #16 (methyl); **b** lignin signals #2 (etherified syringyls), #3 (non-etherified syringyls, guaiacyls), and #15 (methoxyl)

160 °C/0.3 MPa. Up to 180 °C/0.3 MPa, there was a downward slight trend in the relative intensity of signal #4, which was an evidence of β–O–4 bonds cleavage. The resonances corresponding to cellulose had not appeared to change markedly. All the results highly agreed with the previous study.

The changes of the signals #1 and #16 at 172 and 21 ppm assigned to hemicelluloses could be perceived only after a very close inspection of the signals, as well as the signals #2, #3 and #15 assigned to lignin. To secure the previous observations, elaborate quantitative analyses of the NMR spectra were carried out. For hemicelluloses, the focus was set on resonances arising from carbonyl and methyl carbons of acetyl groups (signals #1 and #16, respectively). Similarly, the C-3 and C-5 of syringyls in etherified (signal #2), non-etherified structures (signals #3) and methoxyl groups (signal #15) were used to characterize the modifications in the lignin structure. The normalized peak area evolution

of signals assigned to the carbons of hemicellulose acetyls groups was given in Fig. 13a. Concerning lignin degradation, data were reported in Fig. 13b. As was shown in Fig. 13, hemicelluloses started to loose acetyl groups above 160 °C. It could be concluded that the signals from C-3 and C-5 of syringyl units in etherified structures and the one from methoxyl carbons had a similar tendency. In contrast, the normalized peak areas of signal #3 (C-3 and C-5 of syringyls in non-etherified structures and guaiacyls C-3 and C-4) had a trend in an opposite way from the two others. This could indicate that demethoxylation was actually the dominant mechanism above 160 °C. Demethoxylation of syringyls was expected to lead to an increase of guaiacyls which contributed to signal #3. That was in agreement with above.

Conclusion

Our results indicated that transformation of the material induced by this treatment lead to increased lignin and extractives, as well as a decrease in the contents of holocellulose and α-cellulose. XPS spectroscopy results showed the hemicelluloses and celluloses could be strongly affected by the atmosphere in the oven during the treatment. In relative terms, the lignin was not very sensitive to the heating process to some extent. Solid-state NMR results showed that different degree of transformations of the polymers related to deacetylation of hemicelluloses, demethoxylation of lignin and changes in the cellulose structure had been brought by heat treatment.

References

1. He M-J, Zhang J, Li Z, Li M-L (2016) Production and mechanical performance of scrimber composite manufactured from poplar wood for structural applications. J Wood Sci 62:429–440
2. Yu H-X, Fang C-R, Xu M-P, Guo F-Y, Yu W-J (2015) Effects of density and resin content on the physical and mechanical properties of scrimber manufactured from mulberry branches. J Wood Sci 61:159–164
3. Guo X, Lin Y, Na B, Liang X, Ekevad M, Ji F, Huang L (2016) Evaluation of physical and mechanical properties of fiber-reinforced poplar scrimber. BioResources 12:43–55
4. He M, Tao D, Li Z, Li M (2016) Mechanical behavior of dowel-type joints made of wood scrimber composite. Materials 9:581
5. Fu B, Li X, Yuan G, Chen W, Pan Y (2014) Preparation and flame retardant and smoke suppression properties of bamboo-wood hybrid scrimber filled with calcium and magnesium nanoparticles. J Nanomater 1:3
6. Rahayu I, Denaud L, Marchal R, Darmawan W (2015) Ten new poplar cultivars provide laminated veneer lumber for structural application. Ann For Sci 72:705–715
7. Abdolzadeh H, Doosthoseini K, Karimi AN, Enayati AA (2011) The effect of acetylated particle distribution and type of resin on physical and mechanical properties of poplar particleboard. Eur J Wood Wood Prod 69:3–10
8. Zanuttini R, Nicolotti G, Cremonini C (2003) Poplar plywood resistance to wood decay agents: efficacy of some protective treatments in the light of the standard ENV 12038. Ann For Sci 60:83–89
9. Yoshihara H (2011) Bending properties of medium-density fiberboard and plywood obtained by compression bending test. For Prod J 61:56–63
10. Nuopponen M, Vuorinen T, Jämsä S, Viitaniemi P (2003) The effects of a heat treatment on the behaviour of extractives in softwood studied by FTIR spectroscopic methods. Wood Sci Technol 37:109–115
11. Tuong VM, Li J (2010) Changes caused by heat treatment in chemical composition and some physical properties of acacia hybrid sapwood. Holzforschung 65:67–72
12. Windeisen E, Strobel C, Wegener G (2007) Chemical changes during the production of thermo-treated beech wood. Wood Sci Technol 41:523–536
13. Bhuiyan MTR, Hirai N, Sobue N (2000) Changes of crystallinity in wood cellulose by heat treatment under dried and moist conditions. J Wood Sci 46:431–436
14. Melkior T, Jacob S, Gerbaud G, Hediger S, Le Pape L, Bonnefois L, Bardet M (2012) NMR analysis of the transformation of wood constituents by torrefaction. Fuel 92:271–280
15. Boonstra MJ, Pizzi A, Ohlmeyer M, Paul W (2006) The effects of a two stage heat treatment process on the properties of particleboard. Eur J Wood Wood Prod 64:157–164
16. Garcia RA, Riedl B, Cloutier A (2008) Chemical modification and wetting of medium density fibreboard produced from heat-treated fibres. J Mater Sci 43:5037–5044
17. Brischke C, Welzbacher CR, Brandt K (2007) Quality control of thermally modified timber: interrelationship between heat treatment intensities and CIE $L^*a^*b^*$ color data on homogenized wood samples. Holzforschung 61:17–22
18. He W, Song J, Wang T (2017) Effect of heat oil treatment on bamboo scrimber properties. J For Eng 2:15–19
19. Cai J, Li T (2009) Effects of high temperature heat treatment on the physical mechanical properties of the compressed poplar lumber. J For Eng 23:104–106
20. Meng F-d, Yu Y-l, Zhang Y-m, Yu W-j, Gao J-m (2016) Surface chemical composition analysis of heat-treated bamboo. Appl Surf Sci 371:383–390
21. Hembree DM, Smyrl HR (1989) Anomalous dispersion effects in diffuse reflectance infrared fourier transform spectroscopy: a study of optical geometries. Appl Spectrosc 43:267–274
22. GB/T 2677.10 (1995) Fibrous raw material-determination of holocellulose. Chinese Standard Association, Beijing, pp 220–223
23. GB/T 744 (1989) Pulps-determination of a-cellulose. Chinese Standard Association, Beijing, pp 156–158
24. GB/T 2677.8 (1994) Fibrous raw material-determination of acid-insoluble lignin. Chinese Standard Association, Beijing, pp 213–215
25. GB/T 2677.4 (1993) Fibrous raw material-determination of water solubility. Chinese Standard Association, Beijing, pp 204–206
26. GB/T 2677.5 (1993) Fibrous raw material-determination of one percent sodium hydroxide solubility. Chinese Standard Association, Beijing, pp 207–209
27. GB/T 2677.6 (1993) Fibrous raw material-determination of solvent extractives. Chinese Standard Association, Beijing, pp 210–211

28. Xu X, Tang Z, Liang Y, Zhang L, Zeng M (2009) Comparison of the volatile constituents of different parts of cortex magnolia of ficinalis by GC–MS combined with chemometric resolution method. J Sep Sci 20:3466–3472

29. Massiot D, Fayon F, Capron M, King I, Le Calve S, Alonso B (2002) Modelling one- and two-dimensional solid-state NMR spectra. Magn Res Chem 40:70–76

30. Yin SC (1996) Wood Science. Chinese Forestry Publishing House, Beijing

31. Kang HY (2006) Effect of drying methods on the discoloration of three major domestic softwood species in Korea. For Stud China 8:48–50

32. Huang X, Kocaefe D, Kocaefe Y (2012) A spectrocolorimetric and chemical study on color modification of heat-treated wood during artificial weathering. Appl Surf Sci 258:5360–5369

33. Esteves B, Pereira H (2008) Wood modification by heat treatment: a review. BioResources 4:370–404

34. González-Peña MM, Curling SF, Hale MD (2009) On the effect of heat on the chemical composition and dimensions of thermally-modified wood. Polym Degrad Stabil 94:2184–2193

35. Dubey MK, Pang S, Walker J (2012) Changes in chemistry, color, dimensional stability and fungal resistance of *Pinus radiata* D. Don wood with oil heat-treatment. Holzforschung 66:49–57

36. Bourgois J, Guyonnet R (1988) Characterization and analysis of torrefied wood. Wood Sci Technol 22:143–155

37. Manninen A-M, Pasanen P, Holopainen JK (2002) Comparing the VOC emissions between air-dried and heat-treated Scots pine wood. Atmos Environ 36:1763–1768

38. Esteves B, Graca J, Pereira H (2008) Extractive composition and summative. Chemical analysis of thermally treated eucalypt wood. Holzforschung 62(3):344–351

39. Esteves B, Videira R, Pereira H (2011) Chemistry and ecotoxicity of heat-treated pine wood extractives. Wood Sci Technol 45:661–676

40. Brito J, Silva F, Leão M, Almeida G (2008) Chemical composition changes in eucalyptus and pinus woods submitted to heat treatment. Bioresour Technol 99:8545–8548

41. Kumar R, Singh S, Singh OV (2008) Bioconversion of lignocellulosic biomass: biochemical and molecular perspectives. J Ind Microbiol Biot 35:377–391

42. Inari GN, Petrissans M, Lambert J, Ehrhardt J, Gérardin P (2006) XPS characterization of wood chemical composition after heat-treatment. Surf Interface Anal 38:1336–1342

43. Kazayawoko M, Balatinecz J, Sodhi R (1999) X-ray photoelectron spectroscopy of maleated polypropylene treated wood fibers in a high-intensity thermokinetic mixer. Wood Sci Technol 33:359–372

44. Ding T, Peng W, Li T (2017) Mechanism of color change of heat-treated white ash wood by means of FT-IR and XPS analyses. J For Eng 2:25–30

45. Sinn G, Reiterer A, Stanzl-Tschegg SE (2001) Surface analysis of different wood species using X-ray photoelectron spectroscopy (XPS). J Mater Sci 36:4673–4680

46. Hua X, Kaliaguine S, Kokta B, Adnot A (1993) Surface analysis of explosion pulps by ESCA Part 1. Carbon (1s) spectra and oxygen-to-carbon ratios. Wood Sci Technol 27:449–459

47. Kamdem D, Riedl B, Adnot A, Kaliaguine S (1991) ESCA spectroscopy of poly (methyl methacrylate) grafted onto wood fibers. J Appl Polym Sci 43:1901–1912

48. Kocaefe D, Huang X, Kocaefe Y, Boluk Y (2013) Quantitative characterization of chemical degradation of heat-treated wood surfaces during artificial weathering using XPS. Surf Interface Anal 45:639–649

49. Inari GN, Pétrissans M, Dumarcay S, Lambert J, Ehrhardt J, Šernek M, Gérardin P (2011) Limitation of XPS for analysis of wood species containing high amounts of lipophilic extractives. Wood Sci Technol 45:369–382

50. Gérardin P, Petrič M, Petrissans M, Lambert J, Ehrhrardt JJ (2007) Evolution of wood surface free energy after heat treatment. Polym Degrad Stabil 92:653–657

51. Gao N, Li A, Quan C (2013) TG-FTIR and Py-GC/MS analysis on pyrolysis and combustion of pine sawdust. J Anal Appl Pyrol 100:26–32

52. Bardet M, Emsley L, Vincendon M (1997) Two-dimensional spin-exchange solid-state NMR studies of 13 C-enriched wood. Solid State Nucl Mag 8:25–32

53. Gil A, Neto CP (1999) Solid-state NMR studies of wood and other lignocellulosic materials. Annu Rep NMR Spectro 37:75–117

54. Wen J, Chen T, Sun R (2017) Research progress on separation and structural analysis of lignin in lignocellulosic biomass. J For Eng 2:76–84

55. Maunu S (2002) NMR studies of wood and wood products. Prog Nucl Mag Res Sp 40:151–174